applied sciences

MDPI

Article

X-ray Visualization and Quantification Using Fibrous Color Dosimeter Based on Leuco Dye

Phu Phong Vo [1], Hoan Ngoc Doan [1], Kenji Kinashi [2,*], Wataru Sakai [2], Naoto Tsutsumi [2] and Dai Phu Huynh [3]

1 Graduate school of Science and Technology, Kyoto Institute of Technology, Matsugasaki, Sakyo, Kyoto 606-8585, Japan; vpphu94@gmail.com (P.P.V.); ngochoandoan@gmail.com (H.N.D.)
2 Faculty of Materials Science and Engineering, Kyoto Institute of Technology, Matsugasaki, Sakyo, Kyoto 606-8585, Japan; wsakai@kit.ac.jp (W.S.); tsutsumi@kit.ac.jp (N.T.)
3 Polymer Research Center, Faculty of Materials Technology, HoChiMinh City University of Technology, Vietnam National University, HoChiMinh City 700000, Vietnam; hdphu@hcmut.edu.vn
* Correspondence: kinashi@kit.ac.jp; Tel.: +81-075-724-7809

Received: 4 May 2020; Accepted: 25 May 2020; Published: 29 May 2020

Abstract: A polystyrene (PS)-based fibrous color dosimeter, comprising a color former based on 2-(phenylamino)-6-(dipentylamino)-3-methylspiro[9*H*-xanthene-9,3′-phthalide] (Black305) fluoran leuco dye and a 2-(4-methoxystyryl)-4,6-bis(trichloromethyl)-1,3,5-triazine (MBTT) photoacid generator, was developed for visual detection of X-ray doses of 15 Gy and higher. The composite fiber was produced by using a centrifugal spinning method, and the obtained composite fiber exhibited a stable and uniform morphology with a fiber diameter of 10 μm or less and had sufficient mechanical strength. As an example of practical application, we successfully processed the composite fiber into an apron and clearly and visually confirmed that the color change from yellow to black occurs on the surface of the fabric under X-ray exposure.

Keywords: centrifugal spinning; forcespinning; fibrous color dosimeter; leuco dyes; photoacid generator; X-ray visualization

1. Introduction

In recent years, radiotherapy has made great strides, and it is now possible to intensively irradiate only cancer cells with radiation and to suppress the effects on surrounding healthy cells as much as possible. Besides this, it is well-known that amounts of radiation doses have a harmful impact; however, small amounts of radiation doses have another aspect of stimulating various activities of the human body as physiological stimulation (radiation hormesis effect [1,2]). In other words, radiation workers need to accurately measure and manage radiation doses, especially workers working at nuclear power plants, who must always manage their doses. In general, Geiger–Muller counters or semiconductor radiation detector devices have been used for detecting weak radiation. In facilities handling radiation, workers entering the controlled area must carry radiation meters and manage external exposure doses during the working time. Various types of personal dosimeters, such as fluorescent glass dosimeters [3,4], thermoluminescent dosimeters (TLD) [5–8], photostimulated luminescence dosimeters (PSL) [9–11], film badges [12–14], ionization chamber dosimeters [15–17], electronic dosimeters [18–20], GafChromic film dosimetry [21,22], and fiber-like systems dosimeters [23,24], are currently available and the appropriate type of dosimeter is used according to the purpose of use and function. Among the abovementioned personal dosimeters, fluorescent glass dosimeters are currently the most widely used personal dosimeters. However, the fluorescent glass dosimeters require a dedicated reading device to measure the radiation exposure dose and have a fatal disadvantage in that the radiation exposure dose

cannot be known immediately. This is because the fluorescent glass dosimeters use a mechanism to convert the radiation dose obtained using silver-activated phosphate glass into UV-excited fluorescence. Therefore, to overcome these problems, it is necessary to develop a new system that differs from existing radiation dosimeters and can visually, intuitively, and reliably measure the radiation exposure dose [25,26].

In a previous study, we proposed a composite resin dosimeter (CRD) consisting of 2-(4-methoxystyryl)-4,6-bis(trichloromethyl)-1,3,5-triazine (MBTT) as the photoacid generator, 2-(phenylamino)-6-(dipentylamino)-3-methylspiro[9*H*-xanthene-9,3′-phthalide] (Black305) as the color former, and cerium-doped yttrium aluminium perovskite $YAlO_3$:Ce (YAP:Ce) as the scintillator, that changes its color from yellow to thermally stable black upon monochromic X-ray exposure in the range of 18–170 Gy at a wavelength of 0.154 nm [27]. A mechanism for the color change of the CRD film under the X-ray exposure doses was also proposed. The YAP:Ce scintillator powder in the CRD film absorbs the X-ray radiation and then emits the ultraviolet light inside the film. A free radical $Cl^{\bullet}$ is released from the MBTT that absorbs the ultraviolet light, and a photoacid-generating reaction occurs to produce a proton (H^+). The H^+ reacts with the Black305 to open a lactone ring and eventually change the color of the material to black. However, as described above, the proposed composite material contained the YAP:Ce powder in the film, so the flexibility of the material was poor, and it was difficult to process the composite material into a fibrous form.

Recently, fiber centrifugal spinning (or force spinning) has been used to fabricate fibers on the micro or nanoscale [28–30]. This method has high productivity and low cost and does not depend on the conductivity of the polymer solution, unlike the alternative technique of electrospinning. The centrifugal spinning process uses the centrifugal force arising from the high-speed rotation of a spinneret and exploits the properties of the polymer solution such as viscoelasticity and mass transfer characteristics to produce micro/nanofibers with controlled fiber diameter. Additionally, it is well known that several parameters of the centrifugal spinning process, e.g., collector distance, internal nozzle diameter, and type of solvent, affect the structure of the final fiber [31–33].

We propose a fibrous color dosimeter with enhanced flexibility using only the photoacid generator MBTT and Black305. We call it a leuco-based fibrous color dosimeter (fibrous color dosimeter) to distinguish it from the previously reported CRD. This study also discusses the sensitivity of the fibrous color dosimeters under X-ray exposure from the viewpoint of chemical kinetics.

2. Materials and Methods

2.1. Materials

All of the chemicals were commercially available and were used as received. Polystyrene (PS) pellets (M_w = 252,000 g mol^{-1}) and tetrahydrofuran were purchased from the Wako Chemical Co. The fluoran leuco dye 2-(phenylamino)-6-(dipentylamino)-3-methylspiro[9*H*-xanthene-9,3′-phthalide] (Black305) was purchased from the Fukui Yamada Chemical Co. and used as the color former. The 2-(4-methoxystyryl)-4,6-bis(trichloromethyl)-1,3,5-triazine (MBTT) was purchased from the Sigma-Aldrich Co., and used as the photoacid generator.

2.2. Prepare the Leuco-Based Color Dosimeter

The compositions of polystyrene (PS) and tetrahydrofuran (THF) were fixed at 10.0 and 35.5 by weight, and the composition ratio of MBTT and Black305 was varied in the range of 1.0−3.0 by weight, respectively. The PS at a given ratio was dissolved in THF at room temperature and homogenized entirely using a planetary centrifugal mixer (ARE-310, Thinky Co., Tokyo, Japan) operating at 2000 rpm with polyethylene balls (1/2 in.) for 30 min. The mixtures of MBTT and Black305 were stirred in THF, and then added to the PS solution, and the mixture was further stirred for 4 h. The composite fibers were prepared using a build-up centrifugal spinning system with a modified centrifuge separator (Tomy MC150, Tomy Seiko Co., Tokyo, Japan). The centrifugal spinning system consisted of a 32 mm

needle-based spinneret equipped with two blunt needles (inner diameter of 160 µm, and shaft length of 5 mm) and was rotated by an AC motor at speeds ranging from 0 to 15,000 rpm. The feeding rate of the polymer solution was controlled to be 100 mL h^{-1} by a syringe pump (KDS-100, KD Scientific Co., Holliston, MA, USA). In this study, the rotational speed and collection distance were fixed at 15,000 rpm and 10 cm, respectively, based on the spinning conditions of the previous study [27]. The obtained fibers were dried under a vacuum at room temperature and stored in the dark. All procedures, including sample preparation, spinning, storage, and characterizations, were conducted in the darkroom.

2.3. Characterization

The viscosity of each PS solution consisting of MBTT and Black305 was measured using a vibrionic viscometer (SV-1A, A&D Co., Tokyo, Japan) at 25 °C. The measurement was repeated at least three times to obtain the average viscosity. The morphology of the composite fibers was characterized using a scanning electron microscope (SEM) (S-3000N, Hitachi Co., Tokyo, Japan). Fiber diameters and distribution ($N = 200$) were determined from the SEM image (300× magnification), using the ImageJ image processing software (National Institutes of Health, Montgomery County, MD, USA). UV-vis reflectance spectra were recorded using a multichannel spectrophotometer (HSU-100, Asahi Spectra Co., Tokyo, Japan). An X-ray radiation source (HW-100W, Hitex Co., Osaka, Japan) with a W target was used to generate continuous X-ray radiation and was operated at 70 kV and 7 mA. The radiation dose of the radiating X-rays per unit time was estimated to be 0.71 Gy min^{-1} by the change in the absorbance of a Fricke solution [19,20] (Figure S1). The optical images of the composite fibers associated with the color changes during the exposure were taken by a digital camera (TG-3, OLYMPUS Co., Tokyo, Japan), and the chromaticity differences (ΔE) were estimated using the Photoshop CC software package (Adobe Systems Co., San Jose, CA, USA). The ΔE was evaluated using a CIE $L^*a^*b^*$ color model:

$$\Delta E = \sqrt{(\Delta L)^2 + (\Delta a)^2 + (\Delta b)^2} \quad (1)$$

where ΔE is the chromaticity difference, ΔL is the lightness difference, Δa is the red/green difference, and Δb is the yellow/blue difference. The dose-response curves were established based on a model in the previous study to estimate the sensitivity to the X-ray dose at $\Delta E = 10$. The fibrous specimens used for the X-ray exposure test were cut using a cutting blade with a diameter of 20 mm, were covered with a lead plate (100 × 100 × 1 mm) with a hole of 5 mm, and were placed in the continuous X-ray exposure apparatus. The mechanical properties of the fibrous specimens were determined using a universal tensile testing machine (TENSION RFT-1210, A&D Co., Tokyo, Japan) with a cell load of 100 N, test speed of 0.5 mm s^{-1}, and gauge length of 10 mm. The pieces of the fibrous specimens were cut with a cutting blade (type 5B in BS ISO 527:2012) and fixed to a mechanical test holder using a double-sided tape. The thickness of the fibrous specimens was determined by a micrometre screw gauge (Mitutoyo 406-250, Mitutoyo, Kanagawa, Japan). The mechanical tests were performed at least five times in the atmosphere at a temperature of 22 ± 2 °C and RH of 35 ± 5%.

3. Results and Discussion

In the centrifugal spinning process, the morphologies of the obtained fibers were significantly affected by various parameters. In the previous study, the bead-free fibers were successfully prepared using the following spinning conditions: PS/THF ratio of 10.0/35.5 *w*/*w*, rotational speed of 15,000 rpm, needle inner diameter of 160 µm, and collection distance of 10 cm [29]. The dependence of the Black305 concentration on the fiber morphology and fiber diameter was evaluated based on the above spinning conditions. Three kinds of PS solutions were prepared by fixing the MBTT concentration to 1.0 by weight and varying the Black305 concentration, as listed in Table 1. Figure 1 shows the SEM images and the fiber diameters of the composite fibers prepared in the conditions specified in Table 1. The viscosities of the PS solutions with the different concentrations of Black305 were in the 148–150 mPa s range. The viscosities of the polymer solutions were not significantly affected by the concentration of

the added Black305, and the composite fibers prepared with these PS solutions show approximately the same diameter of 9 μm. Moreover, each of the obtained composite fibers is a bead-free fiber, indicating that the PS solutions during the centrifugal spinning process did not exhibit the Plateau–Rayleigh instability when ejected from the nozzle, suggesting a cylindrical polymer jet [24]. The effect of the increasing concentration of MBTT on the morphology and sensitivity for the fibrous color dosimeters was also investigated. The concentration of Black305 was fixed at 30 wt% and three PS solutions with different MBTT concentrations were prepared. The measured viscosities of the PS solutions with different MBTT concentrations were in the range of 149–151 mPa s. These results indicate that the fiber diameters of the composite fibers are controlled predominantly by the viscosity of the PS solutions, implying that the additives, such as Black305 and MBTT, are uniformly dispersed in the composite fibers. The viscosities of the PS solutions and the fiber diameters for the obtained composite fibers are summarized in Table 1. The ATR-FTIR spectra of the composite fibers show that composite fibers prepared by the centrifugal spinning method consists of MBTT and Black305 (Figure S2).

Table 1. Experimental conditions, viscosities of the polystyrene (PS) solutions, and fiber diameters.

MBTT/Black305	PS (g)	MBTT (g)	Black305 (g)	THF (g)	Viscosity (mPa s)	Fiber Diameter (μm)
1.0/1.0 *w/w*	10.0	1.0	1.0	35.5	148.40 ± 0.55	9.16 ± 2.49
1.0/2.0 *w/w*	10.0	1.0	2.0	35.5	150.20 ± 1.50	9.20 ± 2.21
1.0/3.0 *w/w*	10.0	1.0	3.0	35.5	149.40 ± 1.15	8.85 ± 2.23
2.0/3.0 *w/w*	10.0	2.0	3.0	35.5	150.60 ± 1.35	8.61 ± 3.01
3.0/3.0 *w/w*	10.0	3.0	3.0	35.5	151.40 ± 0.90	9.58 ± 3.25

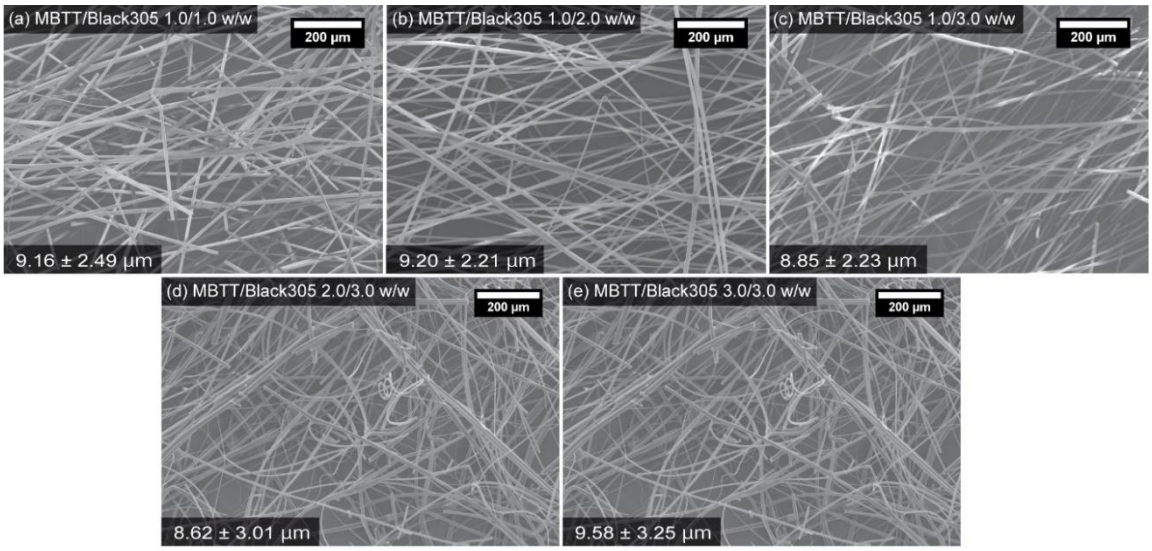

Figure 1. SEM images for the fibrous color dosimeters using the composite fibers prepared using the conditions specified in Table 1.

The dose-response curves for the fibrous color dosimeters based on the composite fibers with the different Black305 concentrations were obtained by plotting the chromaticity difference (ΔE) versus the exposure dose at an exposure rate of 0.71 Gy min^{-1}. All of the experimental assays were performed at room temperature (RT; 20 °C). The obtained plots are shown in Figure 2. The X-ray dosages in these plots were determined using the Fricke solution. The grey areas on the curve indicate the maximum and minimum values of the error. In this study, we defined the maximum sensitivity as the chromaticity difference of 10 or higher because the color changes of 10 or higher can be recognized by the naked eye. The change of color is based on the chromaticity difference ΔE with respect to the exposure dose; all of the fibrous color dosimeters exhibited a good response. However, the ΔEs of the fibrous color dosimeters prepared using the composite fibers with the low concentrations of Black305 corresponding

to the MBTT/Black305 1.0/1.0 and 2.0/2.0 *w*/*w* samples were insufficient, because the obtained ΔE values are below 10 at any dosages, meaning these color changes color cannot be visually identified in this region. On the other hand, based on the sensitivity criterion, a sufficient sensitivity of 33.28 Gy @ ΔE = 10 was obtained for the fibrous color dosimeter with the MBTT/Black305 ratio of 1.0/3.0 *w*/*w*. Consequently, it is suggested that the Black305 concentration should be at least 30 wt% for the MBTT concentration of 10 wt% for recognizing the color change of the fibrous color dosimeter. In addition, an examination of the morphologies of the composite fibers also shows that these fibers are bead-free, as was found for the experiments in which the dependence on the Black305 concentration was examined. These results suggest that the viscosity of the PS solution controls the fiber morphology regardless of the concentrations of Black305 and MBTT. When the fibrous color dosimeters obtained using increased concentration of MBTT were examined, it was found that the rise of the dose-response curves was improved, and as a result, the sensitivity was successfully improved to 15.36 Gy @ ΔE = 10. It is suggested that this improvement in sensitivity is based on the reaction mechanism described below that was first described in our previous study [27]. A kinetic model considering a two-step consecutive first-order reaction for the color-changing in this fibrous color dosimeter was proposed as follows

$$\mathrm{MBTT} \xrightarrow{X-ray} \mathrm{MBTT} + \mathrm{Cl}$$
$$\mathrm{Cl} + \mathrm{RH\ (polystyren)} \xrightarrow{k_1} H^+Cl^- + R$$
$$H^+Cl^- + \mathrm{Black305\ (colorless)} \xrightarrow{k_2} \mathrm{Black305-H\ (black)} + Cl^-$$

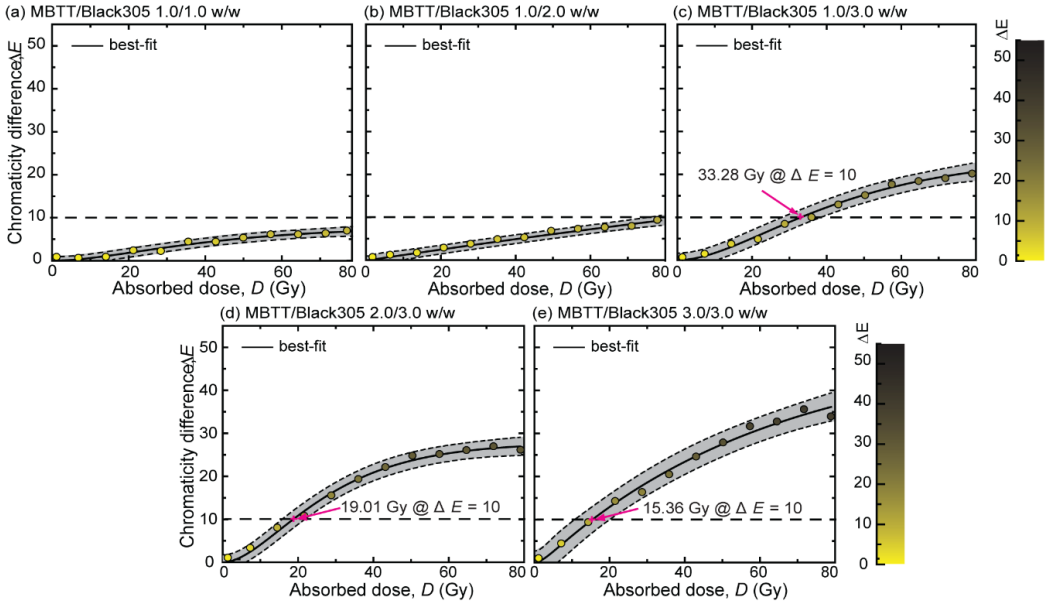

Figure 2. Dose-response curves at 20 °C for the fibrous color dosimeters using the composite fibers prepared under the conditions specified in Table 1. The black dashed line indicates the point at which the color change can be visually observed. The color bar indicates the color tone corresponding to ΔE.

At the first step in the reaction scheme, the MBTT in the fibrous color dosimeter directly absorbed the X-rays. Most of the irradiated X-rays are lost due to transmission; however, the MBTT absorbs a small fraction of the irradiated X-rays because of its X-ray absorption property, and radical generation occurs to produce a free radical (Cl•). Subsequently, the generated Cl• immediately reacts with the polymer matrix RH (polystyrene) to generate a proton in the second step. This radical-generating reaction has been reported by Pawlowski et al. [34]. The produced H^+ diffuses and reacts with Black305 to cleave the lactone ring of the colorless leuco-form in Black305, and give the black colored dye-form Black305-H in the third step. As a result, the absorbed exposure area gradually changes to a black

color according to the absorbed dose, and this color change can be visually observed. In the previous study, we developed a composite resin dosimeter (CRD) film containing a scintillator YAP:Ce that emits ultraviolet light inside the film that was the driving force for the radical generation from the MBTT. However, this CRD film contains a powdery inorganic scintillator YAP:Ce in the film and is unsuitable for use as a fabric because of its low mechanical strength.

Furthermore, the sensitivity can be improved by heating based on the proposed thermodynamic mechanism. Figure S3 shows the thermal gravimetric analysis (TGA) curves of the fibrous color dosimeter with a MBTT/Black305 ratio at 3.0/3.0 *w*/*w*, Black305, MBTT, and PS fiber in air. During the first stage of the TGA, the fibrous color dosimeter showed a slight weight loss due to the presence of water at approximately 100 °C. In addition, no weight loss was observed up to 230 °C due to decomposition derived from the MBTT, and some weight losses of the materials contained in the fiber were observed in high temperature regions of 360 °C and 530 °C. Based on the result of the TGA, it was suggested that the thermal stability of the PS-based fibrous color dosimeters with MBTT/Black305 would be guaranteed up to the glass-transition temperature of PS of 100 °C. That is, if the color changing reaction processes thermodynamically, generally, increasing temperature can promote reaction activity (Figure S4); however, this thermodynamic property of the fibrous color dosimeters will be one of the issues in practical application because making a quantitative assessment of radiation exposure doses requires maintaining a constant temperature during use. Therefore, it is pointed out that the recommended operating temperature of the fibrous color dosimeter will be room temperature from the viewpoint of thermal stability. The humidity of the ambient can affect the dosimeter response as well [35]. Therefore, the effect of humidity on dose-response of the fibrous color dosimeter will need to be considered in the future.

We conducted a preliminary experiment of X-ray exposure visualization using a fabric based on the fibrous color dosimeter (3.0/3.0 *w*/*w*), which presents photographic images of color changes during X-ray exposure at room temperature (RT; 20 °C). The leftmost photograph in Figure 3a shows the fabric before X-ray exposure. The color of the fabric before X-ray exposure is based on the absorption characteristics of MBTT. The circular black colors on the fabrics indicate the actual color change due to the X-ray exposure, and the dose dependence of the coloration is shown in Figure 3b. In addition, the black circles on the fabrics completely trace the shape of a window formed on a lead plate placed on the fabric. Figure 3b exhibits the UV−visible reflectance spectral changes of the color of the fabric during X-ray exposure at an interval of 20 Gy. Before the X-ray exposure, the broad reflection band where the reflection bands of PS and MBTT overlap appears in the region <532 nm. Under X-ray exposure, the color of the fabric gradually changes to black, and the reflection spectra with a peak of 610 nm are attributed to the colored zwitterionic form of Black305 [25]. Consequently, the reflectivity of the fabric changed drastically from 58% for yellow to 32% for black. Photographs of the fabric before and after an X-ray exposure dose of 80 Gy are presented in Figure 3c. An important property of the fabric is that its color changes can be uniformly confirmed as a whole, which indicates that the MBTT and Black305 dispersed entirely and would not form aggregates in the fabric. For future applications on the personal wearable dosimeter, the mechanical properties of the fabric were investigated as well. The mechanical properties of the fabric must be strong enough to build a wearable device. Figure 3d shows the stress–strain curve of the fibric. As a result, the maximum tensile stress and elongation at maximum tensile stress for the fabric are 0.36 ± 0.01 MPa and 1.3 ± 0.4%, respectively, and the properties are consistent with a nonwoven fabric derived from PS fibers [23]. Therefore, the mechanical strength of the fabric has a sufficient performance as a wearable dosimeter. Finally, a practical demonstration of X-ray visualization using the fabric that was processed into an apron is presented in Figure 3e. We put the fibrous color dosimeter apron on a teddy bear and placed it in inside the X-ray exposure apparatus. Then, we put a lead plate with a "❤" shape hole on the teddy bear to distinguish the contrast between the exposed area and unexposed one. As shown in Figure 3e, the black heart shape area shows the area exposed to 80 Gy of X-ray radiation, and the yellow is the unexposed area.

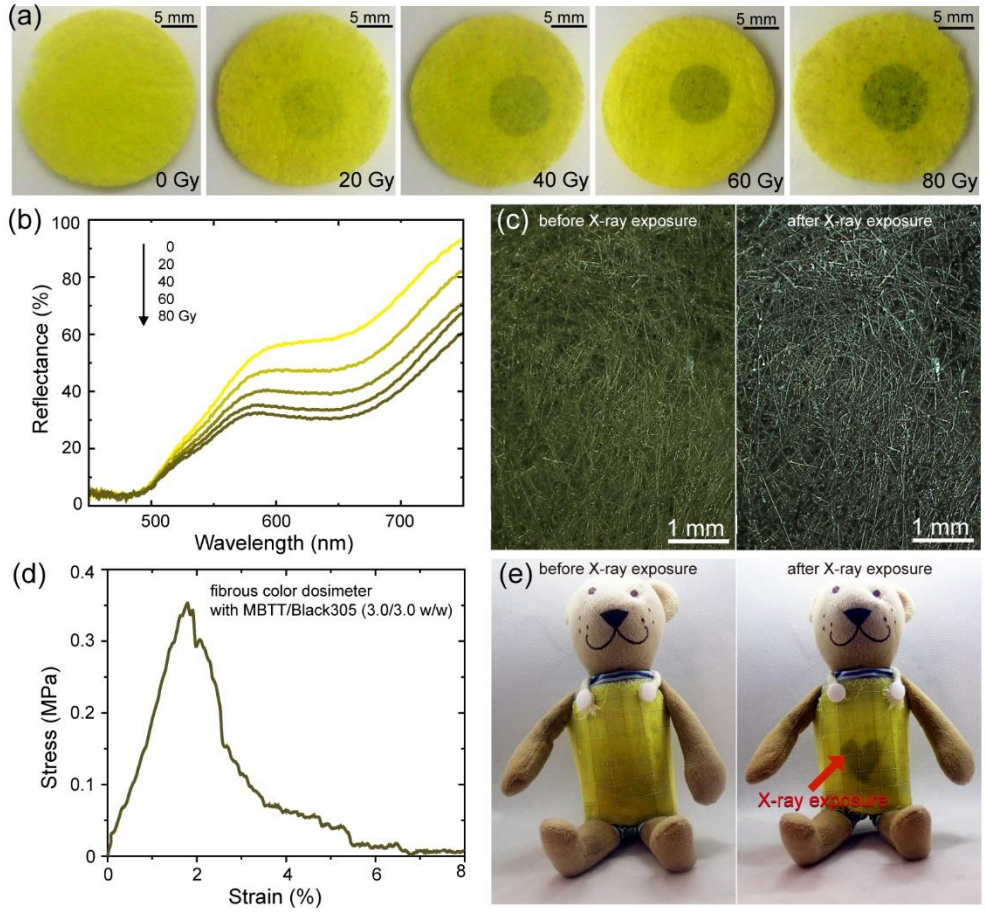

Figure 3. (**a**) Photographs of color changes of the fibrous color dosimeter with a MBTT/Black305 ratio at 3.0/3.0 *w*/*w* for each X-ray exposure dose. Black areas indicate the spot that is irradiated with the X-ray exposure. (**b**) The change in the reflectance spectrum of the fibrous color dosimeter with a MBTT/Black305 ratio at 3.0/3.0 *w*/*w* during X-ray exposure doses. (**c**) Photograph showing the aspect of the fibrous color dosimeter with a MBTT/Black305 ratio at 3.0/3.0 *w*/*w* before and after X-ray exposure for 80 Gy. (**d**) Stress–strain curve of the fibrous color dosimeter. (**e**) Photographs of the clothlike fibrous color dosimeter with a MBTT/Black305 ratio at 3.0/3.0 *w*/*w* (left) before and (right) after X-ray exposure through the lead sheet cut in a "❤" shape.

Consequently, the new fibrous color dosimeters without an inorganic scintillator have the potential to be processed into various shapes, such as clothes, gloves, and so on, due to its sufficient mechanical strength. In addition, when the composite fibers were processed into the apron shape and used, the color change of the apron-shaped dosimeter had an ability to intuitively alert us to the danger of radiation exposure. Furthermore, this color change was irreversible and stable at ambient temperature. In other words, the fibrous color dosimeter using the composite fiber composed of PS, MBTT, and Black305 will be expected to be an alternative to digital dosimeters as a new tool that can recognize the X-ray exposure dose in real-time.

4. Conclusions

The fibrous color dosimeter having the color change sensitivities of 15-33 Gy was successfully prepared by using the centrifugal-spun composite fibers composed of PS, MBTT, and Black305. The fibrous color dosimeter with the maximum sensitivity of 15.36 Gy @ ΔE = 10 was prepared from the composite fiber with a MBTT/Black305 ratio at 3.0/3.0 *w*/*w*. The mechanical strength of the composite fiber with the maximum sensitivity was sufficient for processing, and it could be processed

into an apron shape. The apron-shaped fibrous color dosimeter changes color depending on the X-ray exposure dosage, which allows visual confirmation of the presence or absence of radioactive materials.

Supplementary Materials: The following are available online at http://www.mdpi.com/2076-3417/10/11/3798/s1, Figure S1: Absorbance spectra of the Fricke dosimeter before and after X-ray exposure. Figure S2: ATR-FTIR spectra of the composite fibers, MBTT (photoacid), leuco dye Black 305, and PS fibers. Figure S3: TGA thermograms of the fibrous color dosimeter with a MBTT/Black305 ratio at 3.0/3.0 *w*/*w*, Black305, MBTT, and PS fibers in air. Figure S4: Dose-response curves of the fibrous color dosimeters made of the composite fibers consist of MBTT/Balck305 3.0/3.0 by weight at different temperatures (a) 20 °C, (b) 40 °C, (c) 60 °C. The color bar signifies the color tone corresponding to ΔE. The black broken line indicates the point at which color change can be visually observed.

Author Contributions: Conceptualization, P.P.V., H.N.D., and K.K.; investigation, P.P.V. and H.N.D.; methodology, P.P.V.; project administration, K.K.; supervision, K.K.; writing—original draft, P.P.V., H.N.D.; writing—review and editing, K.K., W.S., N.T., and D.P.H. All authors have read and agreed to the published version of the manuscript.

Funding: This research was supported by Grants-in-Aid from the JSPS core-to-Cor Program, B-Asia-Africa Science Platforms, and Kansai Research Foundation for Technology Promotion.

Acknowledgments: P.P.V. greatly acknowledges the Ministry of Education, Sports, and Culture of Japan (MEXT) scholarship provided by the Japanese Government for his studies at the Kyoto Institute of Technology.

Conflicts of Interest: The authors declare no conflicts of interest.

References

1. Calabrese, E.J. Hormesis: Changing view of the dose-response, a personal account of the history and current status. *Mutat. Res. Rev. Mutat. Res.* **2002**, *511*, 181–189.
2. Calabrese, E.J.; Baldwin, L.A. Radiation hormesis and cancer. *Hum. Ecol. Risk Assess. An Int. J.* **2002**, *8*, 327–353. [CrossRef]
3. Farah, K.; Mejri, A.; Hosni, F.; Ben Ouada, H.; Fuochi, P.G.; Lavalle, M.; Kovács, A. Characterization of a silicate glass as a high dose dosimeter. *Nucl. Instrum. Methods Phys. Res. Sect. A Accel. Spectrometers Detect. Assoc. Equip.* **2010**, *614*, 137–144. [CrossRef]
4. Moon, Y.M.; Kim, H.J.; Kwak, D.W.; Kang, Y.R.; Lee, M.W.; Ro, T.I.; Kim, J.K.; Jeong, D.H. Effective dose measurement for cone beam computed tomography using glass dosimeter. *Nucl. Eng. Technol.* **2014**, *46*, 255–262.
5. Del Sol Fernández, S.; García-Salcedo, R.; Sánchez-Guzmán, D.; Ramírez-Rodríguez, G.; Gaona, E.; De León-Alfaro, M.A.; Rivera-Montalvo, T. Thermoluminescent dosimeters for low dose X-ray measurements. *Appl. Radiat. Isot.* **2016**, *107*, 340–345. [CrossRef] [PubMed]
6. D'Amorim, R.A.P.O.; Teixeira, M.I.; Caldas, L.V.E.; Souza, S.O. Physical, morphological and dosimetric characterization of the Teflon agglutinator to thermoluminescent dosimetry. *J. Lumin.* **2013**, *136*, 186–190.
7. Nelson, V.; McLean, D.; Holloway, L. Thermoluminescent dosimetry (TLD) for megavoltage electron beam energy determination. *Radiat. Meas.* **2010**, *45*, 698–700. [CrossRef]
8. Moscovitch, M.; Horowitz, Y.S. Thermoluminescent materials for medical applications: LiF:Mg,Ti and LiF:Mg,Cu,P. *Radiat. Meas.* **2006**, *41* (Suppl. 1), 71–77.
9. Moritake, T.; Matsumaru, Y.; Takigawa, T.; Nishizawa, K.; Matsumura, A.; Tsuboi, K. Dose measurement on both patients and operators during neurointerventional procedures using photoluminescence glass dosimeters. *Am. J. Neuroradiol.* **2008**, *29*, 1910–1917. [CrossRef]
10. Yukihara, E.G.; McKeever, S.W. Optically stimulated luminescence (OSL) dosimetry in medicine. *Phys. Med. Biol.* **2008**, *53*, 351. [CrossRef]
11. Mehta, S.K.; Sengupta, S. Photostimulated thermoluminescence of Al2O3(Si, Ti) and its application to ultraviolet radiation dosimetry. *Phys. Med. Biol.* **1978**, *23*, 471–480. [CrossRef] [PubMed]
12. Diffey, B. The early days of personal solar ultraviolet dosimetry. *Atmosphere* **2020**, *11*, 125. [CrossRef]
13. Jabeen, A.; Munir, M.; Khalil, A.; Masood, M.; Akhter, P. Occupational exposure from external radiation used in medical practices in Pakistan by film badge dosimetry. *Radiat. Prot. Dosim.* **2010**, *140*, 396–401. [CrossRef]
14. Ali, J.B.; Jacobson, R.E. The use of diazo film as a film badge dosimeter. *J. Photogr. Sci.* **1980**, *28*, 172–176. [CrossRef]
15. O'Brien, D.J.; Roberts, D.A.; Ibbott, G.S.; Sawakuchi, G.O. Reference dosimetry in magnetic fields: Formalism and ionization chamber correction factors. *Med Phys.* **2016**, *43*, 4915–4927. [CrossRef]

16. Martin, C.J. An evaluation of semiconductor and ionization chamber detectors for diagnostic X-ray dosimetry measurements. *Phys. Med. Biol.* **2017**, *52*, 4465–4480. [CrossRef]
17. Bouchard, H.; Seuntjens, J. Ionization chamber-based reference dosimetry of intensity modulated radiation beams. *Med. Phys.* **2004**, *31*, 2454–2465. [CrossRef]
18. Guimarães, M.C.; Da Silva, T.A. Characterization of a medical X-ray machine for testing the response of electronic dosimeters in pulsed radiation fields. *Radiat. Phys. Chem.* **2014**, *104*, 321–323. [CrossRef]
19. Takahashi, M.; Sekiguchi, M.; Miyauchi, H.; Tachibana, H.; Yoshizawa, M.; Kato, T.; Yamaguchi, A. Performance of the Hp(10) and Hp(0.07) measurable electronic pocket dosimeter for gamma- and beta-rays. *J. Nucl. Sci. Technol.* **2008**, *45*, 225–228. [CrossRef]
20. Rosenfeld, A.B. Electronic dosimetry in radiation therapy. *Radiat. Meas.* **2006**, *41* (Suppl. 1), 134–153. [CrossRef]
21. Desroches, J.; Bouchard, H.; Lacroix, F. Technical note: Potential errors in optical density measurements due to scanning side in EBT and EBT2 gafchromic film dosimetry. *Med. Phys.* **2010**, *37*, 1565–1570. [CrossRef] [PubMed]
22. Martin, C.J.; Gentle, D.J.; Sookpeng, S.; Loveland, J. Application of gafchromic film in the study of dosimetry methods in CT phantoms. *J. Radiol. Prot.* **2011**, *31*, 389–409. [CrossRef] [PubMed]
23. Kozicki, M.; Sąsiadek, E.; Kadlubowski, S.; Dudek, M.; Karbownik, I. Radiation sensitive polyacrylonitrile microfibres doped with PDA Nano-Particles. *Radiat. Phys. Chem.* **2020**, *169*, 107751. [CrossRef]
24. Kozicki, M.; Sąsiadek, E.; Karbownik, I.; Maniukiewicz, W. Doped Polyacrylonitrile Fibres as UV radiation sensors. *Sens. Actuators B Chem.* **2015**, *213*, 234–243. [CrossRef]
25. Tsuchida, H.; Nakamura, R.; Kinashi, K.; Sakai, W.; Tsutsumi, N.; Ozaki, M.; Okabe, T. Radiation-induced colour changes in a spiropyran/BaFCl:Eu^{2+}/polystyrene composite film and nonwoven fabric. *New J. Chem.* **2016**, *40*, 8658–8663. [CrossRef]
26. Kinashi, K.; Iwata, T.; Tsuchida, H.; Sakai, W.; Tsutsumi, N. Composite Resin Dosimeters: A New Concept and Design for a Fibrous Color Dosimeter. *ACS Appl. Mater. Interfaces* **2018**, *10*, 11926–11932. [CrossRef]
27. Iwata, T.; Kinashi, K.; Doan, H.N.; Vo, P.P.; Sakai, W.; Tsutsumi, N. Leuco-based composite resin dosimeter film. *ACS Omega* **2019**, *4*, 9946–9951. [CrossRef]
28. Vo, P.; Doan, H.; Kinashi, K.; Sakai, W.; Tsutsumi, N.; Huynh, D. Centrifugally spun recycled PET: Processing and characterization. *Polymers* **2018**, *10*, 680. [CrossRef]
29. Doan, H.N.; Nguyen, D.K.; Vo, P.P.; Hayashi, K.; Kinashi, K.; Sakai, W.; Huynh, D.P.; Tsutsumi, N. Facile and scalable fabrication of porous polystyrene fibers for oil removal by centrifugal spinning. *ACS Omega* **2019**, *4*, 15992–16000. [CrossRef]
30. Badrossamay, M.R.; McIlwee, H.A.; Goss, J.A.; Parker, K.K. Nanofiber assembly by rotary jet-spinning. *Nano Lett.* **2010**, *10*, 2257–2261. [CrossRef]
31. Obregon, N.; Agubra, V.; Pokhrel, M.; Campos, H.; Flores, D.; De la Garza, D.; Mao, Y.; Macossay-Torres, J.; Alcoutlabi, M. Effect of polymer concentration, rotational speed, and solvent mixture on fiber formation using forcespinning®. *Fibers* **2016**, *4*, 20.
32. Golecki, H.M.I.; Yuan, H.; Glavin, C.; Potter, B.; Badrossamay, M.R.; Goss, J.A.; Phillips, M.D.; Parker, K.K. Effect of solvent evaporation on fiber morphology in rotary jet spinning. *Langmuir* **2014**, *30*, 13369–13374. [PubMed]
33. Valipouri, A.; Ravandi, S.A.H.; Pishevar, A.R. A novel method for manufacturing nanofibers. *Fibers Polym.* **2013**, *14*, 941–949. [CrossRef]
34. Pawlowski, G.; Dammel, R.; Przybilla, K.J.; Röschert, H.; Spiess, W. Novel photoacid generators: Key components for the progress of chemically amplified photoresist systems. *J. Photopolym. Sci. Technol.* **1991**, *4*, 389–402. [CrossRef]
35. Faheem, E.; El Ahdal, M.A.; Protection, R. High dose film dosimeter based on a mixture of M-Cresol purple and tetrabromo phenolphthalein ethyl ester dyed poly (vinyl alcohol). *Egypt. J. Radiat. Sci. Appl.* **2015**, *28*, 49–60.